Published in final edited form as:
J Neural Eng. 2012 August ; 9(4): 046005. doi:10.1088/1741-2560/9/4/046005.

Improved spatial targeting with directionally segmented deep brain stimulation leads for treating essential tremor

Maureen Keane[1,*], **Steve Deyo**[1,*], **Aviva Abosch**[2,3], **Jawad A. Bajwa**[4,5], and **Matthew D. Johnson**[1,3,†]

[1]Department of Biomedical Engineering, University of Minnesota, Minneapolis, USA

[2]Department of Neurosurgery, University of Minnesota, Minneapolis, USA

[3]Institute for Translational Neuroscience, University of Minnesota, Minneapolis, USA

[4]Capistrant Center for Parkinson's Disease and Movement Disorders, Bethesda Hospital, Saint Paul, MN, USA

[5]National Neuroscience Institute, King Fahad Medical City, Riyadh, Saudi Arabia

Abstract

Deep brain stimulation (DBS) in the ventral intermediate nucleus of thalamus (Vim) is known to exert a therapeutic effect on postural and kinetic tremor in patients with essential tremor. For DBS leads implanted near the caudal border of Vim, however, there is an increased likelihood that one will also induce paresthesia side-effects by stimulating neurons within the sensory pathway of the ventral caudal (Vc) nucleus of thalamus. The aim of this computational study was to 1) investigate the neuronal pathways modulated by therapeutic, sub-therapeutic, and paresthesia-inducing DBS settings in three patients with essential tremor, and 2) determine how much better of an outcome could have been achieved had these patients been implanted with a DBS lead containing directionally-segmented electrodes (dDBS). Multi-compartment neuron models of the thalamocortical, cerebellothalamic, and medial lemniscal pathways were first simulated in the context of patient-specific anatomies, lead placements, and programming parameters from three ET patients who had been implanted with Medtronic 3389 DBS leads. The models showed that in these patients, complete suppression of tremor was associated most closely with activating an average of 62% of the cerebellothalamic afferent input into Vim (n=10), while persistent paresthesias were associated with activating 35% of the medial lemniscal tract input into Vc thalamus (n=12). The dDBS lead design demonstrated superior targeting of the cerebello-thalamo-cortical pathway, especially in cases of misaligned DBS leads. Given the close proximity of Vim to Vc thalamus, the models suggest that dDBS will enable clinicians to more effectively sculpt current through and around thalamus in order to achieve a more consistent therapeutic effect without inducing side effects.

Keywords

Deep brain stimulation; essential tremor; computational modeling; segmented; electrode

[†]Address correspondence to: Matthew D. Johnson, Department of Biomedical Engineering, University of Minnesota, 7-105 NHH, 312 Church Street SE, Minneapolis, MN, 55455, ph: (612)-626-6492, fax: (612)-626-6583, john5101@umn.edu.
[*]These authors contributed equally to the work

Conflict of Interest: None

Introduction

Essential tremor (ET), characterized by postural and kinetic tremors (4-12 Hz) primarily in the upper extremities and head (Whaley et al. 2007), is the most common adult movement disorder, affecting 0.4-4% of the population (Louis et al. 1998). While pharmacological therapies are known to reduce tremor symptoms, approximately one-third of ET patients are refractory to medication (Zesiewicz et al. 2010). For these patients, deep brain stimulation (DBS) can be an effective surgical therapy (Lozano 2000); however, the efficacy of this neurosurgical procedure is highly dependent on proper placement of the DBS lead in or near the cerebellar-receiving area of thalamus (ventral intermediate nucleus, Vim).

Previous studies have noted that improvement in tremor symptoms can be obtained by stimulating through electrodes either within Vim (Benabid et al. 1991; Kobayashi et al. 2010) or slightly ventral to Vim (Barbe et al. 2011a; Herzog et al. 2007; Sandvik et al. 2011). These clinical observations suggest that there may be multiple therapeutic stimulation targets for managing essential tremor, including the thalamocortical tract from Vim to primary motor cortex, as well as the cerebellothalamic tract projecting into Vim. In the first case, DBS is thought to override neuronal tremor-burst activity in Vim (Hua et al. 1998) by generating a regular, albeit higher frequency of spike activity in Vim (Birdno et al. 2008; McIntyre et al. 2004). In the latter case, DBS is thought to drive high frequency activity into Vim thereby impeding the facilitation of tremor-burst activity through Vim (Birdno et al. 2011).

The typical DBS lead trajectory is made along the border of Vim and the pallidal-receiving area of thalamus (nucleus ventral oral posterior, Vop) so as to prevent suprathreshold currents from spreading posterior to the sensory nucleus of thalamus (ventral caudal, Vc). Correct placement of the DBS lead can typically be identified not only by suppression of tremor in the contralateral upper limb but also by transient paresthesias induced in the fingers and/or face (Benabid et al. 2004). Posterior placements of the stimulating electrode within Vim can modulate a significant portion of Vc, inducing persistent paresthesias at low voltages of stimulation (Kuncel et al. 2008). Leads placed medially are known to elicit intraoral paresthesias with stimulation, while paresthesias in the leg usually indicate that the lead is positioned too lateral. These boundaries are important considerations for neurosurgical targeting of DBS leads because an estimated two mm difference in electrode placement versus intended target has been reported for DBS implants that have been guided with intraoperative microelectrode recordings (McClelland et al. 2005). Given the potential for these targeting errors with stereotactic neurosurgical implantation of DBS leads, there is a strong need for lead designs that enable clinicians to more precisely modulate the appropriate neuronal pathways to suppress tremor without evoking untoward side-effects.

DBS leads with directionally-segmented electrodes may enable improved steering of current in the brain (Martens et al. 2011), but the practical application of these devices to brain targets for essential tremor has not yet been investigated. In this study, we developed a patient-specific, computational framework to compare 1) clinical improvement in tremor to model predictions of the percentage of Vim efferent and afferent projections modulated during DBS, and 2) emergence of paresthesias to model predictions of the proportion of Vc efferent and afferent projections modulated during DBS. We then used the patient-specific models to evaluate a novel directionally-segmented DBS lead for improving the overall therapeutic outcome of a patient whose DBS lead was implanted near Vc thalamus.

Materials and Methods

Human Subjects

This study involved retrospective computational modeling and image analysis of three patients who had been clinically diagnosed with medication-refractory essential tremor with average duration of 35 years. Each patient had been implanted with DBS lead(s) to suppress upper extremity tremor (Table 1). Two patients received a unilateral left DBS implant, while the third patient received bilateral DBS implants (Medtronic 3389 leads with electrodes of 1.5 mm height and 0.5 mm spacings). Imaging and clinical DBS programming data were de-identified prior to analysis. Tremor severity was evaluated on a clinical rating scale by a trained movement disorders neurologist before and during the DBS programming session. Consent for this research study was obtained from established patients at the Capistrant Center for Parkinson's Disease and Movement Disorders at Bethesda Hospital per HealthEast Care System protocols and the University of Minnesota Institutional Review Board.

Anatomical Surface Reconstructions

Computational models of the neuronal pathways putatively activated by DBS were created for each subject. Pre-operative volumetric MR images were first aligned in Talairach coordinate space. Coronal MR slices containing thalamus were then matched to corresponding slices within a human brain atlas (Mai et al. 2008). Because the clinical MRI resolution obtained from the 3T magnet contained insufficient contrast to segment nuclei within thalamus, a composite imaging and warped brain atlas approach was undertaken. Using a series of anatomically relevant landmarks, each brain atlas image was warped to conform to the patient MR slice using the software, Edgewarp (Figure 1A-C). The warped brain atlas images were then traced in Rhinoceros, a non-uniform rational basis spline program, to create a series of planar contours, each containing estimates of the anatomical borders of thalamic nuclei, including Vim and Vc. These contours were then lofted in three dimensions to create surface renderings of each thalamic nucleus. DBS leads were localized within the computational model space by co-registering post-operative CT images to the pre-operative MR images, using the software Analyze.

Thalamic Neuron Morphologies and Projections

Vim and Vc thalamic volumes were populated with a neuron template consisting of an anatomically realistic, 3D multi-compartment cable model of a thalamocortical (TC) relay cell (Figure 1D). Because no study to date has created a digital morphological reconstruction of a complete TC neuron from a human or non-human primate, we used a modified version of a rodent TC relay cell model template consisting of a soma and dendritic tree spanning 250 μm (Destexhe et al. 1998). We justified the use of this model given that the cell template morphology and spread of the dendritic arbors were within the range of values reported in histological studies of the primate thalamus (Jones 2007). We modeled the axonal trajectories of these cells based upon histological studies localizing these fiber tracts to the non-human primate primary motor cortex (Hoover and Strick 1999) and somatosensory cortex (Darian-Smith et al. 1999; Kultas-Ilinsky et al. 2003). The efferent tracts to cortex coursed along a medial-ventral to lateral-dorsal angle in the coronal plane and posterior-ventral to anterior-dorsal angle in the sagittal plane (Kakei et al. 2001). Five hundred copies of the neuron template were randomly distributed within Vim and again within Vc, allowing for a 10 degree randomized angle of rotation within both coronal and sagittal planes.

Cerebellothalamic afferents to Vim and lemniscal afferents to Vc were also constructed with multi-compartment axonal cable models (n=500 each). These tracts were based on the

warped brain atlas from each patient with fibers coursing at an angle of 45° with the intercommissural line in the coronal plane. In the sagittal plane, the entrance to Vim and Vc thalamus followed a 60° angle with the intercommissural plane (Gallay et al. 2008). Template afferents extending into the dorsal half of each thalamic nucleus were constructed from a longer cable model than those extending to the ventral half of thalamus. This categorization enabled all afferent models to be enclosed within the anatomical borders of each fiber tract defined by each patient's warped brain atlas.

Predicting Neuronal Responses to DBS

The Vim and Vc efferents and afferents were simulated within the NEURON v7.1 programming environment (Hines and Carnevale 2009). Somatic and dendritic membrane properties were consistent with those defined previously (Destexhe et al. 1998; McIntyre et al. 2004), and included membrane capacitance, linear leakage properties, and nonlinear calcium, sodium, and potassium conductances. Axonal processes consisted of nodes of Ranvier, myelin attachment segments, paranode main segments, and internode segments (Johnson and McIntyre 2008; McIntyre et al. 2004). Vim and Vc afferents were modeled as only axonal processes, given the large distance between the stimulation source and the afferent cell bodies.

A 3D finite element model (FEM) consisting of a tetrahedral mesh was modeled around each DBS lead using COMSOL Multiphysics v4.0. The electric potential in the neural tissue surrounding the lead was modeled within a cylinder of radius 50 mm and height 50 mm, with the outer bound set to ground potential. The tissue surrounding the lead was modeled as a homogenous and isotropic medium, with a conductivity of 0.3 S/m, except for an encapsulation layer at the electrode interface, which was represented by a 0.25 mm thick layer at 0.18 S/m. (Grill and Mortimer 1994; Haberler et al. 2000; Moss et al. 2004). The model assumed ideal electrode behavior and linear scaling of electric fields (Johnson and McIntyre 2008). Each compartment of each neuronal process was then instantiated with a dynamic extracellular membrane potential consistent with the stimulation waveform and scaled according to the FEM solution. Electrical capture of axonal output with DBS was defined by detection of axonal action potentials distal to the stimulation target occurring within 1-3 ms of application of the stimulus and with a probability ≥ 0.8. The patient-specific neuron models of DBS provided a method for comparing spatial activation profiles between a clinical DBS lead with four cylindrical contacts (Medtronic, 3389) and a novel DBS lead with directionally-segmented electrodes (dDBS). The dDBS lead investigated in this study was vertically as well as horizontally segmented, and capable of shifting the spatial activation profile within the brain with sub-millimeter precision. The lead consisted of 16 equally spaced rows with 4 electrode contacts spanning each row. Each annular contact had a diameter of 0.5 mm and spacing between rows of 0.25 mm. The diameter was 1.27 mm, matching the diameter of the Medtronic 3389 lead.

In contrast to the voltage-controlled stimulation delivered through the 3389 DBS lead in the three ET subjects, the dDBS lead was simulated using current-controlled stimulation, which has been shown to facilitate enhanced current steering capabilities (Butson and McIntyre 2008; Martens et al. 2011). We modeled current-controlled stimulation in the case of dDBS simulations in order to accommodate comparisons of this study's results with future studies investigating more complex current steering patterns. In order to facilitate a comparison between cylindrical lead stimulation and dDBS lead stimulation, calibration between voltage and current sources was performed (Figure 2). First, the electric potential surrounding a 1 V source applied to one of the cylindrical electrode contacts was modeled. This voltage distribution was compared to that produced with a variable current source using a test matrix of 400 points extending 9.5 mm horizontally and 9.5 mm vertically from the bounds of the distal contact. The current source magnitude was varied until the mean absolute error of the

difference in test matrix voltage values between the voltage source(s) and current source(s) was minimized. A 2 mA current source produced the lowest mean error between the spatial voltage distributions. Moreover, an equivalent voltage distribution in the surrounding tissue to stimulation through a cylindrical contact in the Medtronic 3389 lead was found to result from stimulating through 2 rows of contacts with the dDBS lead. In this case, the current source was divided between 8 contacts, yielding a current-per-contact of 0.25 mA and a current injection of 0.029 mC/cm^2 per electrode (assuming a 90 μs-long cathodic pulse as applied in the three ET patients).

The stimulus pulse train was consistent with the implantable pulse generator (IPG) setting for each patient (185 Hz, 90 μs cathodic stimulus). The voltage waveform was based on experimental records of a voltage-controlled IPG (Medtronic, Minneapolis, MN), which exhibited a 90 μs cathodic pulse followed by a 400 μs interphase delay and a 3 ms anodic pulse. The signal was filtered in order to account for electrode-tissue capacitive properties (Butson and McIntyre 2005). In the case of current-controlled stimulation through the dDBS lead, the stimulus waveform was scaled from an experimental recording of a constant-current IPG, matching the frequency and pulse-width implemented during clinical programming (Lempka et al. 2010).

Data Analysis

The patient imaging and programming data sets included four DBS lead implants with a total of 50 stimulation parameter sets tested clinically for tremor suppression efficacy and side-effect persistence. Clinical outcomes for each of these settings were grouped into four categories: incomplete improvement (n=4), complete improvement (n=10, 3 of 4 leads), transient paresthesias (n=5), and persistent paresthesias (n=12). Stimulation through Lead 4 was not able to sufficiently suppress tremor in Subject 3; therefore the therapeutic outcome from this lead was not included in the grouped data analysis. The remaining outcomes (n=19), including the report of no improvement and/or no-side effect, were not statistically analyzed. Non-parametric statistical tests were performed given the small sample size. In order to compare the percent neuronal activation, to the categorical treatment effect, the two-sided Mann-Whitney U test was performed at significance level $p<0.05$. This non-parametric approach is used to test whether samples are drawn from the same distribution and have equal medians based on a rank comparison of the data. Because each response variable, or cell type, was treated as an independent sample, tests were performed separately and not corrected for multiple comparisons.

Results

Patient-Specific Modeling Predictions

The computational model predictions were compared with clinical outcome scores for the three lead implants that achieved complete suppression of tremor (Figure 3). As expected, the simulation results showed that driving the axonal output from Vim with high-frequency stimulation was associated with improved therapeutic benefit while activating the axonal output from Vc was associated with the perception of paresthesias. However, the percent activation in both thalamic efferent populations was low (8.7% and 9.9%, respectively). Introducing Vim and Vc afferents into the model was necessary to account for the improvement in tremor and onset of paresthesias in all patients (Figure 4). Complete suppression of tremor was associated with an average of 62.4% (n=10) of the Vim afferents activated by DBS, whereas persistent paresthesias were associated with 35.3% (n=12) of the Vc afferents activated by DBS.

Non-parametric significance tests were performed to compare the median and distribution of neuronal activation looking at the effect of either suppression of tremor or emergence of paresthesias (Figure 3). The null hypothesis was that the data came from the same distribution with equal medians. In comparing the data from incomplete to complete resolution of tremor, the Vim afferents demonstrated near statistical significance ($p=0.05$), while the Vim efferents did not reach significance ($p=0.52$). There was not a statistically significant difference for the progression from transient to persistent paresthesias for the Vc efferents ($p=0.96$) or Vc afferents ($p=0.57$).

Sensitivity Analysis of Lead Placement

While the clinical settings varied electrode configurations along the DBS lead, we next asked the question of how varying the horizontal position of the electrodes would affect the neuronal pathways activated by DBS. Sensitivity to horizontal lead placement was evaluated by simulating DBS in the patient-specific models in which the lead was shifted 1 mm in one of four directions about the plane of the neurosurgical microdrive. This analysis was performed using each subject's final clinical DBS settings. The coordinates of the DBS lead were translated in a positive x and y, and negative x and y direction as shown in Figure 5. The lowest variability in activation was observed for the implant in Subject 2 (Lead 2), in which the patient demonstrated complete resolution of tremor at only 1 V. On the other hand, the largest variability in activation was found for the right implant in Subject 3 (Lead 4), in which complete suppression of tremor was not achieved due to the emergence of low-threshold paresthesias. In this case, the maximum difference in Vc activation with 1-mm displacement was 31% and 9% for Vc afferents and efferents respectively. Moving the position of the lead 1 mm toward Vc resulted in a 182% increase in Vc efferent activation and a 77% increase in Vc afferent activation. These results indicate that for leads placed near the border of Vc, there is a high likelihood that onset of persistent paresthesias may occur at a DBS threshold below that for complete suppression of tremor.

Novel Lead Performance

While three of the DBS implants in this study were able to completely suppress contralateral tremor, there was one case in which DBS programming only achieved minimal benefit due to the emergence of persistent paresthesias with increasing stimulation amplitude (Lead 4). The DBS lead for this patient was programmed with a bipolar stimulation setting in order to limit the tangential activation volume around the DBS lead; nevertheless, the therapeutic benefit on tremor remained less than optimal. This presented an interesting case to evaluate the directionally segmented lead performance in comparison to the standard clinical lead performance. We investigated if better therapy could have been achieved had a dDBS lead been implanted instead of the clinically available cylindrical electrode design (Figure 6).

Five dDBS stimulation configurations were evaluated in terms of their ability to specifically target the cerebello-thalamo-cortical pathway (Vim afferents) without concurrent activation of Vc thalamus. For each of the five dDBS electrode configurations evaluated, a current balance was maintained. The first model (Model A) was designed to closely match the patient's final bipolar electrode configuration through a Medtronic 3389 lead. The dDBS electrode configuration consisted of two rows of cathodic contacts and two rows of anodic contacts, matching the locations of the cathode and anode of the clinical cylindrical lead. Models B-E used an 8-contact cathode arrangement of four rows and two adjacent electrode contacts oriented toward the Vim. Models B and D were designed to have the cathodic contacts facing Vim and the anodic contacts oriented in the opposite direction towards Vc, given the higher activation volumes with cathodic stimulation (McIntyre and Grill 2002). Models C and E were designed to have the cathode surrounded vertically by anodes, all of which faced towards Vim. These settings were chosen to demonstrate the capability of the

segmented lead to activate pathways with fine adjustment based on the individual electrode contact settings. Configurations were constrained to use the same total current as the bipolar case. The results shown in Figure 6 suggest that a more desirable stimulation protocol could be implemented using the new directionally-segmented lead design, resulting in similar Vim activation levels while at the same time avoiding modulation of Vc afferents and efferents. In practice, more complex settings could be applied in order to achieve an optimal therapy.

Discussion

In this study, we developed a patient-specific computational modeling framework to 1) predict the neuronal pathways directly modulated by therapeutic Vim-DBS in essential tremor patients and 2) evaluate a novel DBS lead design aimed at steering current toward those pathways involved in the therapeutic mechanisms of action and away from those pathways associated with untoward side effects.

Model Calibration

The models were first evaluated in the context of each patient's perception of transient and persistent paresthesias across a range of DBS voltage settings. DBS in and near the Vc thalamus is thought to generate somatic sensations (Kuncel et al. 2008), as receptive fields localized within Vc are known to respond to sensory stimulation (Hua et al. 2000). For leads placed near the ventral border of Vim, our results indicated that leads placed too posterior and lateral could lead to activation of the medial lemniscal tract and the perception of paresthesias. The computational models of the patients in our study showed that an activation of 9.9% Vc efferents and 35.3% Vc afferents, on average, was associated with persistent paresthesias. It is important to note, however, that absolute activation percentages are based on the model neurons' excitability, which in turn depends on a variety of model parameter assumptions (Destexhe et al. 1998; McIntyre et al. 2004) that may not fully represent the diverse neuronal dynamics and cellular morphologies present in the brains of patients with essential tremor. It is also important to note that the MRI resolution in our study required image warping of a human brain atlas to each patient's MRI, rather than direct segmentation of nuclei from each patient's MRI. Future work investigating a greater number of patients and utilizing high-field MRI at 7T and above may provide the resolution and contrast to segment individual nuclei within thalamus from the imaging data (Abosch et al. 2010) and to perform high-resolution tractography through diffusion tensor imaging (Lenglet et al. 2012).

Cerebellothalamic Tract Stimulation

Since the leads were localized near the ventral portion of Vim, with at least one electrode contact extending beyond the ventral border of Vim, the model predictions likely favored the hypothesis that activation of the afferent projections into thalamus rather than the efferent output drives therapeutic outcome. Therefore, we cannot conclude that stimulation of the cerebellothalamic tract is a more efficient target than stimulation of the thalamocortical tract as others have hypothesized (Birdno et al. 2011; Blomstedt et al. 2011; Sandvik et al. 2011). However, our results do present evidence that stimulation of the brain region at the level of the cerebellothalamic tract provides a viable explanation for a mechanism of tremor reduction. The model predictions showed greater activation of the cerebellothalamic pathway with increasing suppression of tremor symptoms. Recent DTI studies have shown similar results, where significant connectivity involving the superior cerebellar peduncle was recorded at the location of effective tremor suppression (Klein et al. 2012). It is worth noting that other fiber tracts may also be modulated within this volume of activation, including pallidothalamic fibers, zona incerta projections, and other tracts passing to and from midbrain and brainstem nuclei (Baron et al. 2001; Blomstedt et al. 2009; Gallay

et al. 2008). It is also worth noting that because the cerebellothalamic tract has a cross-sectional area significantly smaller than that of the Vim, as observed in our patient-specific models, smaller amounts of current may be required to achieve a similar therapeutic effect (Hirai et al. 1983). Indeed, using two leads in cases of DBS within the Vim can be necessary to completely resolve tremor symptoms (Foote and Okun 2005; Kobayashi et al. 2010), suggesting a greater activation volume may be necessary within thalamus.

Deep brain stimulation for essential tremor presents a challenge for stereotactic implantation as displacements in ideal implant trajectories on the millimeter scale may result in poor resolution of tremor and possible generation of untoward side-effects. The sensitivity analysis shown in our study demonstrated the importance of precise implantation as millimeter shifts in lead placement can lead to large variations in neuronal activation of both Vim and Vc pathways. These results also suggest that although the Vim may be an effective location for stimulation, the standard cylindrical lead may not suffice for selectively activating the cerebello-thalamo-cortical pathway.

Directionally-Segmented DBS Leads

As such, we investigated the feasibility of using a directionally segmented lead design to enable a more effective therapeutic outcome without inducing paresthesias in a patient with a poorly targeted DBS lead. A previous computational modeling study demonstrated the capacity of a dDBS lead design to enable current steering radially around the lead with sub-millimeter precision (Martens et al. 2011). This type of accuracy would be especially desirable in cases when a DBS lead is inadvertently implanted near the Vim/Vc border. Such was the case for the right implant in Subject 3. The computational models suggested that stimulating through the dDBS lead rather than the standard cylindrical configuration would have led to a better suppression of symptoms. Similar benefits would likely be achieved in other small and complex target regions where directed current steering is desirable, such as in the subthalamic nucleus or the pedunculopontine nucleus.

For some patients, the beneficial effects of Vim-DBS have been observed to decrease gradually over time (Barbe et al. 2011b; Benabid et al. 1996; Blomstedt et al. 2007). Clinicians may choose to increase stimulation amplitude or even implant a second parallel lead in an attempt to regain tremor control; however, this can also lead to adverse side-effects (Yu et al. 2009). Alternatively, stimulation with the dDBS lead explored in this study could provide an efficient method to control the spread of stimulation field to alternative pathways involved in the pathophysiology of essential tremor. The use of patient-specific modeling in the clinic could provide a potential solution to this problem (Butson et al. 2007), as an optimal parameter set can first be chosen based on the models.

Although the dDBS lead may provide improved outcomes in patients with essential tremor, one of the potential challenges will be programming the stimulation settings of such a lead, especially if the patient was implanted with a neurostimulator capable of independent channel, current-controlled stimulation. In our study, only five dDBS lead settings were investigated, though countless more could be tested. Simplifying the DBS parameter space to a few electrode configurations will be an important next step for this type of lead to have a practical impact in clinical practice.

Conclusion

This study illustrates instances in which postural and intention tremor were resolved with stimulation through DBS leads placed near the ventral border of Vim. We found that the inclusion of cerebello-thalamic projections to the Vim thalamus, along with medial lemniscal projections to the Vc thalamus, were necessary to fit the model data to the clinical

results. This finding corroborates previous studies hypothesizing Vim afferents to be a target for relieving tremor (Herzog et al. 2007). For patients with leads positioned near Vc thalamus, a directionally segmented DBS lead design may allow clinicians to better target the cerebello-thalamo-cortical pathway without inducing untoward side effects.

Acknowledgments

This study was supported by the Institute for Engineering in Medicine, and by the College of Science and Engineering and Institute for Translational Neuroscience at the University of Minnesota. We thank Nick Sausen and Allison Connolly for technical assistance. We also thank the Minnesota Supercomputing Institute for providing computational resources that made this work possible.

References

Abosch A, Yacoub E, Ugurbil K, Harel N. An assessment of current brain targets for deep brain stimulation surgery with susceptibility-weighted imaging at 7 tesla. Neurosurgery. 2010; 67:1745–1756. discussion 1756. [PubMed: 21107206]

Barbe MT, Liebhart L, Runge M, Deyng J, Florin E, Wojtecki L, Schnitzler A, Allert N, Sturm V, Fink GR, Maarouf M, Timmermann L. Deep brain stimulation of the ventral intermediate nucleus in patients with essential tremor: stimulation below intercommissural line is more efficient but equally effective as stimulation above. Experimental neurology. 2011a; 230:131–137. [PubMed: 21515262]

Barbe MT, Liebhart L, Runge M, Pauls KA, Wojtecki L, Schnitzler A, Allert N, Fink GR, Sturm V, Maarouf M, Timmermann L. Deep brain stimulation in the nucleus ventralis intermedius in patients with essential tremor: habituation of tremor suppression. Journal of neurology. 2011b; 258:434–439. [PubMed: 20927533]

Baron MS, Sidibe M, DeLong MR, Smith Y. Course of motor and associative pallidothalamic projections in monkeys. The Journal of comparative neurology. 2001; 429:490–501. [PubMed: 11116233]

Benabid, AL.; Lebas, JF.; Grand, S.; Benazzouz, A.; Pollak, P.; Krack, P.; Koudsie, A.; Chabardes, S.; Fraix, V.; Limousin, P.; Pinto, S.; Hoffmann, D.; Ardouin, C.; Funkiewiez, A. Deep brain stimulation for movement disorders. In: Winn, HR., editor. Youmans Neurological Surgery. Philadelphia: Saunders; 2004.

Benabid AL, Pollak P, Gao D, Hoffmann D, Limousin P, Gay E, Payen I, Benazzouz A. Chronic electrical stimulation of the ventralis intermedius nucleus of the thalamus as a treatment of movement disorders. Journal of neurosurgery. 1996; 84:203–214. [PubMed: 8592222]

Benabid AL, Pollak P, Gervason C, Hoffmann D, Gao DM, Hommel M, Perret JE, de Rougemont J. Long-term suppression of tremor by chronic stimulation of the ventral intermediate thalamic nucleus. Lancet. 1991; 337:403–406. [PubMed: 1671433]

Birdno MJ, Kuncel AM, Dorval AD 2nd, Turner DA, Gross RE, Grill WM. Stimulus features underlying reduced tremor suppression with temporally patterned deep brain stimulation. J Neurophysiol. 2011

Birdno MJ, Kuncel AM, Dorval AD, Turner DA, Grill WM. Tremor varies as a function of the temporal regularity of deep brain stimulation. Neuroreport. 2008; 19:599–602. [PubMed: 18388746]

Blomstedt P, Hariz GM, Hariz MI, Koskinen LO. Thalamic deep brain stimulation in the treatment of essential tremor: a long-term follow-up. Br J Neurosurg. 2007; 21:504–509. [PubMed: 17922323]

Blomstedt P, Sandvik U, Fytagoridis A, Tisch S. The Posterior Subthalamic Area in the Treatment of Movement Disorders: Past, Present, and Future. Neurosurgery. 2009; 64:1029–1038. [PubMed: 19487881]

Blomstedt P, Sandvik U, Linder J, Fredricks A, Forsgren L, Hariz MI. Deep brain stimulation of the subthalamic nucleus versus the zona incerta in the treatment of essential tremor. Acta Neurochir (Wien). 2011; 153:2329–2335. [PubMed: 21904970]

Butson CR, Cooper SE, Henderson JM, McIntyre CC. Patient-specific analysis of the volume of tissue activated during deep brain stimulation. NeuroImage. 2007; 34:661–670. [PubMed: 17113789]

Butson CR, McIntyre CC. Current steering to control the volume of tissue activated during deep brain stimulation. Brain Stimul. 2008; 1:7–15. [PubMed: 19142235]

Butson CR, McIntyre CC. Tissue and electrode capacitance reduce neural activation volumes during deep brain stimulation. Clin Neurophysiol. 2005; 116:2490–2500. [PubMed: 16125463]

Darian-Smith C, Tan A, Edwards S. Comparing thalamocortical and corticothalamic microstructure and spatial reciprocity in the macaque ventral posterolateral nucleus (VPLc) and medial pulvinar. The Journal of comparative neurology. 1999; 410:211–234. [PubMed: 10414528]

Destexhe A, Neubig M, Ulrich D, Huguenard J. Dendritic low-threshold calcium currents in thalamic relay cells. J Neurosci. 1998; 18:3574–3588. [PubMed: 9570789]

Foote KD, Okun MS. Ventralis intermedius plus ventralis oralis anterior and posterior deep brain stimulation for posttraumatic Holmes tremor: two leads may be better than one: technical note. Neurosurgery. 2005; 56:E445. discussion E445. [PubMed: 15794849]

Gallay MN, Jeanmonod D, Liu J, Morel A. Human pallidothalamic and cerebellothalamic tracts: anatomical basis for functional stereotactic neurosurgery. Brain structure & function. 2008; 212:443–463. [PubMed: 18193279]

Grill WM, Mortimer JT. Electrical properties of implant encapsulation tissue. Annals of biomedical engineering. 1994; 22:23–33. [PubMed: 8060024]

Haberler C, Alesch F, Mazal PR, Pilz P, Jellinger K, Pinter MM, Hainfellner JA, Budka H. No tissue damage by chronic deep brain stimulation in Parkinson's disease. Annals of neurology. 2000; 48:372–376. [PubMed: 10976644]

Herzog J, Hamel W, Wenzelburger R, Potter M, Pinsker MO, Bartussek J, Morsnowski A, Steigerwald F, Deuschl G, Volkmann J. Kinematic analysis of thalamic versus subthalamic neurostimulation in postural and intention tremor. Brain. 2007; 130:1608–1625. [PubMed: 17439979]

Hirai T, Miyazaki M, Nakajima H, Shibazaki T, Ohye C. The correlation between tremor characteristics and the predicted volume of effective lesions in stereotaxic nucleus ventralis intermedius thalamotomy. Brain. 1983; 106(Pt 4):1001–1018. [PubMed: 6360305]

Hoover JE, Strick PL. The organization of cerebellar and basal ganglia outputs to primary motor cortex as revealed by retrograde transneuronal transport of herpes simplex virus type 1. J Neurosci. 1999; 19:1446–1463. [PubMed: 9952421]

Hua SE, Garonzik IM, Lee JI, Lenz FA. Microelectrode studies of normal organization and plasticity of human somatosensory thalamus. J Clin Neurophysiol. 2000; 17:559–574. [PubMed: 11151975]

Hua SE, Lenz FA, Zirh TA, Reich SG, Dougherty PM. Thalamic neuronal activity correlated with essential tremor. J Neurol Neurosurg Psychiatry. 1998; 64:273–276. [PubMed: 9489548]

Johnson MD, McIntyre CC. Quantifying the neural elements activated and inhibited by globus pallidus deep brain stimulation. J Neurophysiol. 2008; 100:2549–2563. [PubMed: 18768645]

Jones, EG. The thalamus. Cambridge ; New York: Cambridge University Press; 2007.

Kakei S, Na J, Shinoda Y. Thalamic terminal morphology and distribution of single corticothalamic axons originating from layers 5 and 6 of the cat motor cortex. The Journal of comparative neurology. 2001; 437:170–185. [PubMed: 11494250]

Klein JC, Barbe MT, Seifried C, Baudrexel S, Runge M, Maarouf M, Gasser T, Hattingen E, Liebig T, Deichmann R, Timmermann L, Weise L, Hilker R. The tremor network targeted by successful VIM deep brain stimulation in humans. Neurology. 2012; 78:787–795. [PubMed: 22377809]

Kobayashi K, Katayama Y, Sumi K, Otaka T, Obuchi T, Kano T, Nagaoka T, Oshima H, Fukaya C, Yamamoto T, Atsumi H. Effects of electrode implantation angle on thalamic stimulation for treatment of tremor. Neuromodulation : journal of the International Neuromodulation Society. 2010; 13:31–36. [PubMed: 21992762]

Kultas-Ilinsky K, Sivan-Loukianova E, Ilinsky IA. Reevaluation of the primary motor cortex connections with the thalamus in primates. The Journal of comparative neurology. 2003; 457:133–158. [PubMed: 12541315]

Kuncel AM, Cooper SE, Grill WM. A method to estimate the spatial extent of activation in thalamic deep brain stimulation. Clin Neurophysiol. 2008; 119:2148–2158. [PubMed: 18632304]

Lempka SF, Johnson MD, Miocinovic S, Vitek JL, McIntyre CC. Current-controlled deep brain stimulation reduces in vivo voltage fluctuations observed during voltage-controlled stimulation. Clin Neurophysiol. 2010; 121:2128–2133. [PubMed: 20493764]

Lenglet C, Abosch A, Yacoub E, De Martino F, Sapiro G, Harel N. Comprehensive in vivo mapping of the human basal ganglia and thalamic connectome in individuals using 7T MRI. PLoS One. 2012; 7:e29153. [PubMed: 22235267]

Louis ED, Ottman R, Hauser WA. How common is the most common adult movement disorder? estimates of the prevalence of essential tremor throughout the world. Mov Disord. 1998; 13:5–10. [PubMed: 9452318]

Lozano AM. Vim thalamic stimulation for tremor. Archives of medical research. 2000; 31:266–269. [PubMed: 11036177]

Mai, JK.; Paxinos, G.; Voss, T. Atlas of the human brain. New York: Academic Press; 2008.

Martens HC, Toader E, Decre MM, Anderson DJ, Vetter R, Kipke DR, Baker KB, Johnson MD, Vitek JL. Spatial steering of deep brain stimulation volumes using a novel lead design. Clin Neurophysiol. 2011; 122:558–566. [PubMed: 20729143]

McClelland S 3rd, Ford B, Senatus PB, Winfield LM, Du YE, Pullman SL, Yu Q, Frucht SJ, McKhann GM 2nd, Goodman RR. Subthalamic stimulation for Parkinson disease: determination of electrode location necessary for clinical efficacy. Neurosurg Focus. 2005; 19:E12. [PubMed: 16398462]

McIntyre CC, Grill WM. Extracellular stimulation of central neurons: influence of stimulus waveform and frequency on neuronal output. J Neurophysiol. 2002; 88:1592–1604. [PubMed: 12364490]

McIntyre CC, Grill WM, Sherman DL, Thakor NV. Cellular effects of deep brain stimulation: model-based analysis of activation and inhibition. J Neurophysiol. 2004; 91:1457–1469. [PubMed: 14668299]

Moss J, Ryder T, Aziz TZ, Graeber MB, Bain PG. Electron microscopy of tissue adherent to explanted electrodes in dystonia and Parkinson's disease. Brain. 2004; 127:2755–2763. [PubMed: 15329356]

Sandvik U, Lars-Owe K, Anders L, Patric B. Thalamic and subthalamic DBS for essential tremor: where is the optimal target? Neurosurgery. 2011

Whaley NR, Putzke JD, Baba Y, Wszolek ZK, Uitti RJ. Essential tremor: phenotypic expression in a clinical cohort. Parkinsonism & related disorders. 2007; 13:333–339. [PubMed: 17291815]

Yu H, Hedera P, Fang J, Davis TL, Konrad PE. Confined stimulation using dual thalamic deep brain stimulation leads rescues refractory essential tremor: report of three cases. Stereotactic and functional neurosurgery. 2009; 87:309–313. [PubMed: 19641342]

Zesiewicz TA, Chari A, Jahan I, Miller AM, Sullivan KL. Overview of essential tremor. Neuropsychiatr Dis Treat. 2010; 6:401–408. [PubMed: 20856604]

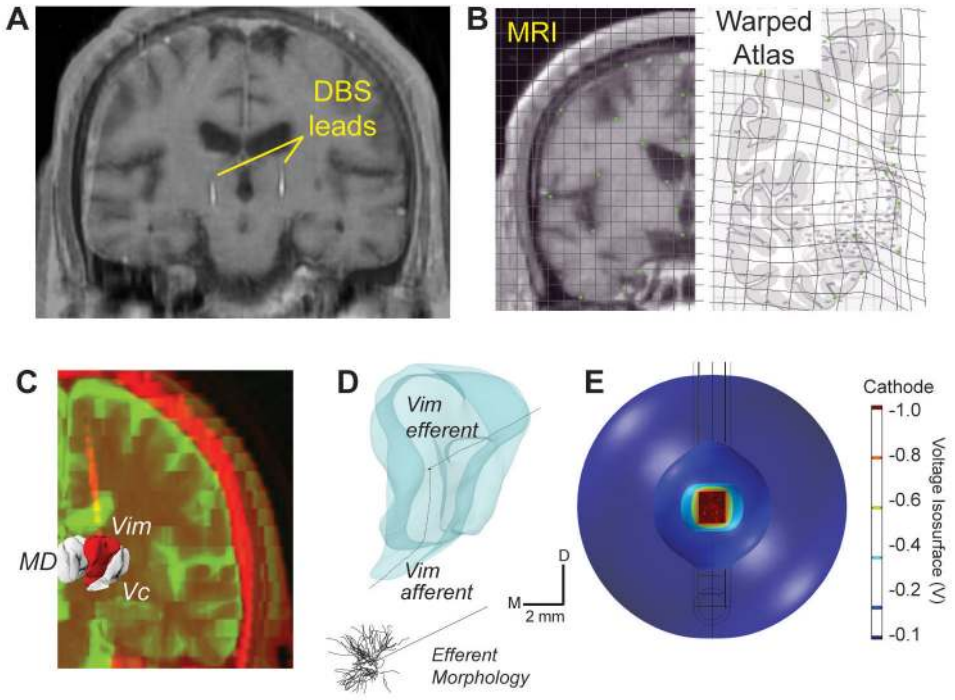

Figure 1.

Patient-specific DBS models for treating essential tremor. **A)** MR data for each patient was matched to a corresponding brain atlas plate based on anatomical landmarks. **B)** A human brain atlas was digitally warped to MR images from each subject. **C)** MRI and CT data were segmented and co-registered to determine lead location. **D)** Each thalamic nucleus was populated with multi-compartment thalamocortical neuron and thalamic afferent axons models. **E)** Finite element analysis involved simulating the voltage distribution in the brain during DBS, as shown for these voltage isosurfaces around a stimulated electrode.

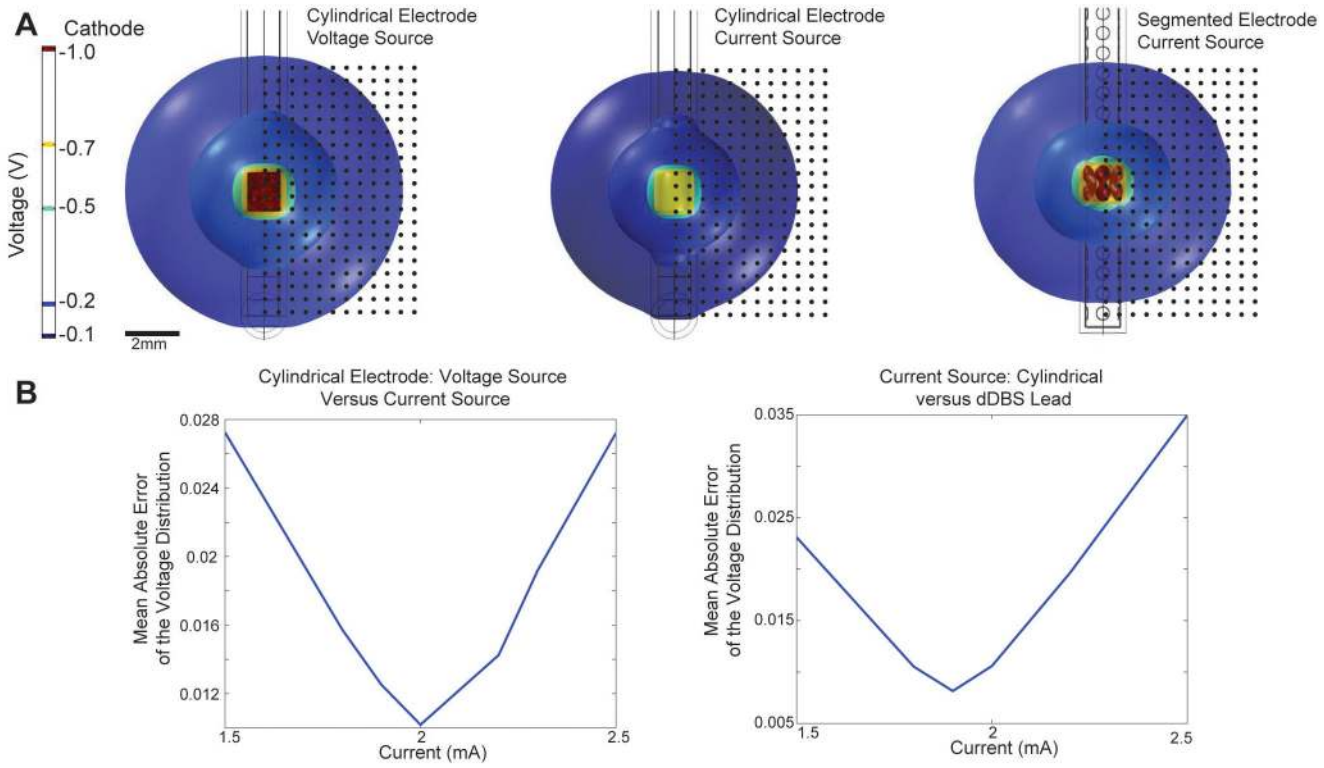

Figure 2.

Finite element model calibration with voltage isosurfaces. **A)** Calibration between voltage- and current-controlled DBS and between stimulation through cylindrical and directionally-segmented electrodes. **B)** Plots of mean error in the spatial voltage profile surrounding each electrode contact during monopolar DBS.

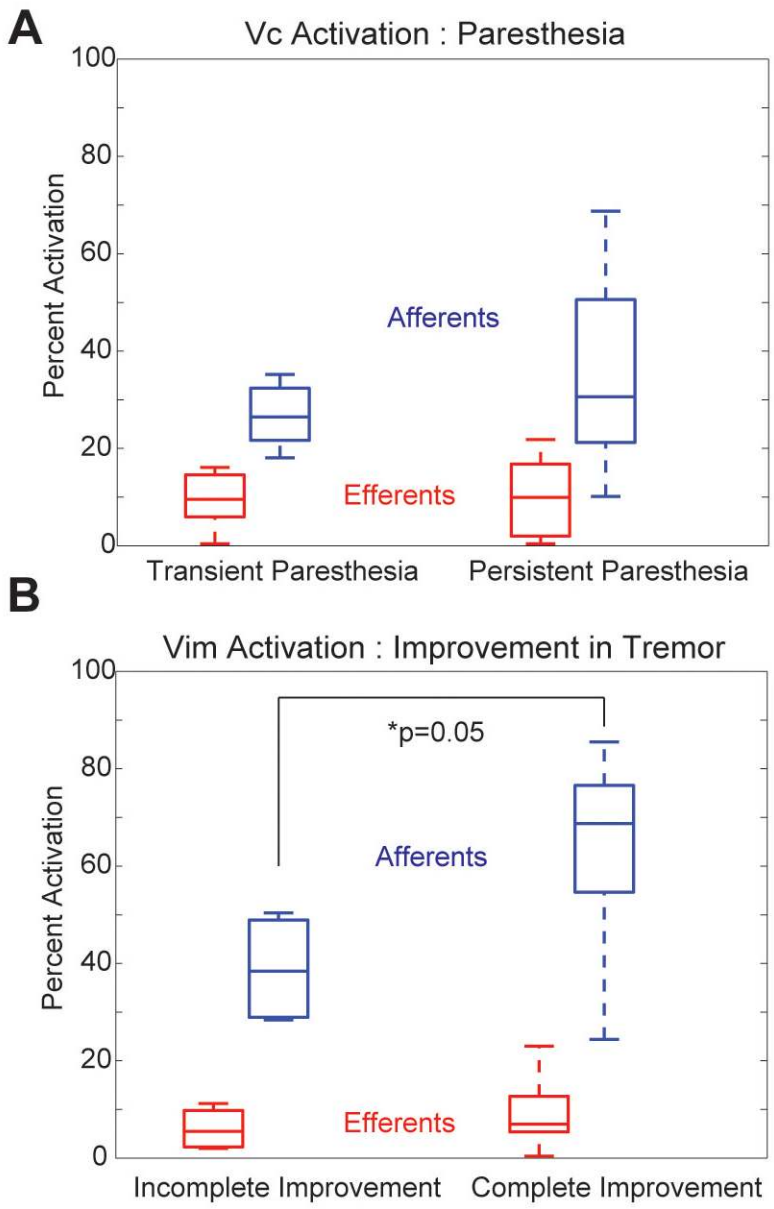

Figure 3.

Grouped analysis of the neuronal pathways activated during DBS programming across the three essential tremor patients. **A)** Percent activation of Vc efferent and afferent projections for outcomes containing transient and persistent paresthesias (n=12 settings). **B)** Percent activation of Vim efferent and afferent projections for outcomes containing incomplete and complete resolution of tremor (n=10 settings).

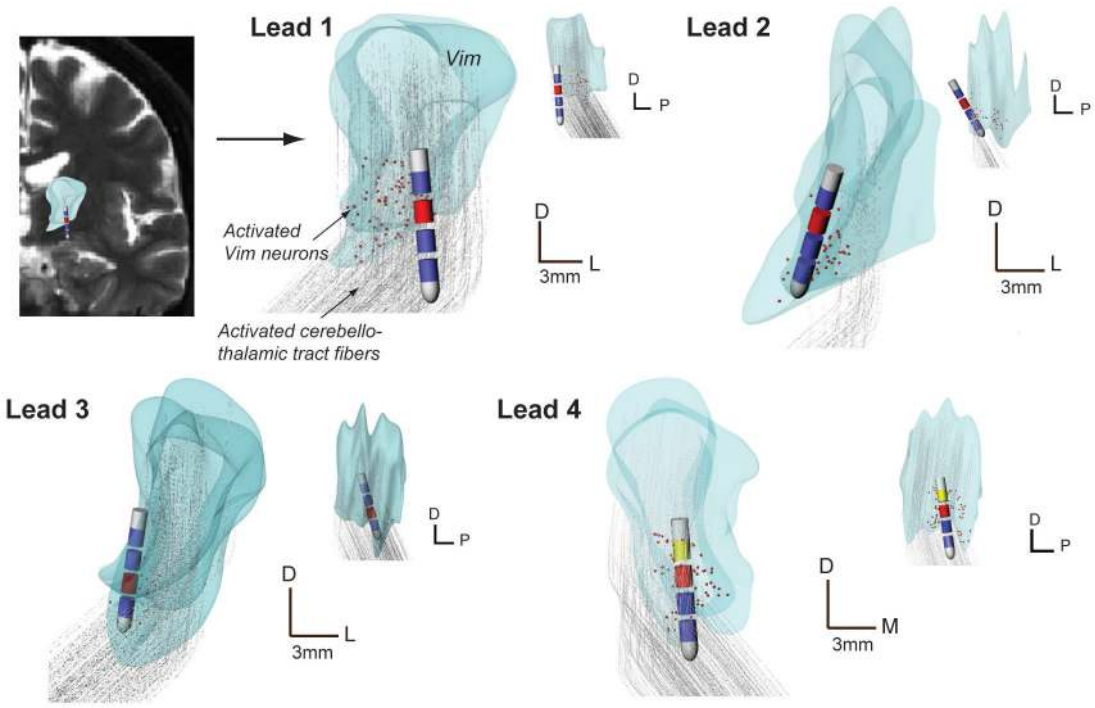

Figure 4.

Patient-specific modeling results for each lead implant. Vim volumes are shown in coronal and sagittal planes and include the co-registered DBS lead positions and active contacts (cathode in red, anode in yellow, IPG was the anode where not shown). Activated Vim neurons (indicated in red) and activated Vim afferents (pathways in gray) are also shown for the clinician-identified best therapy setting. All scale bars: 3mm.

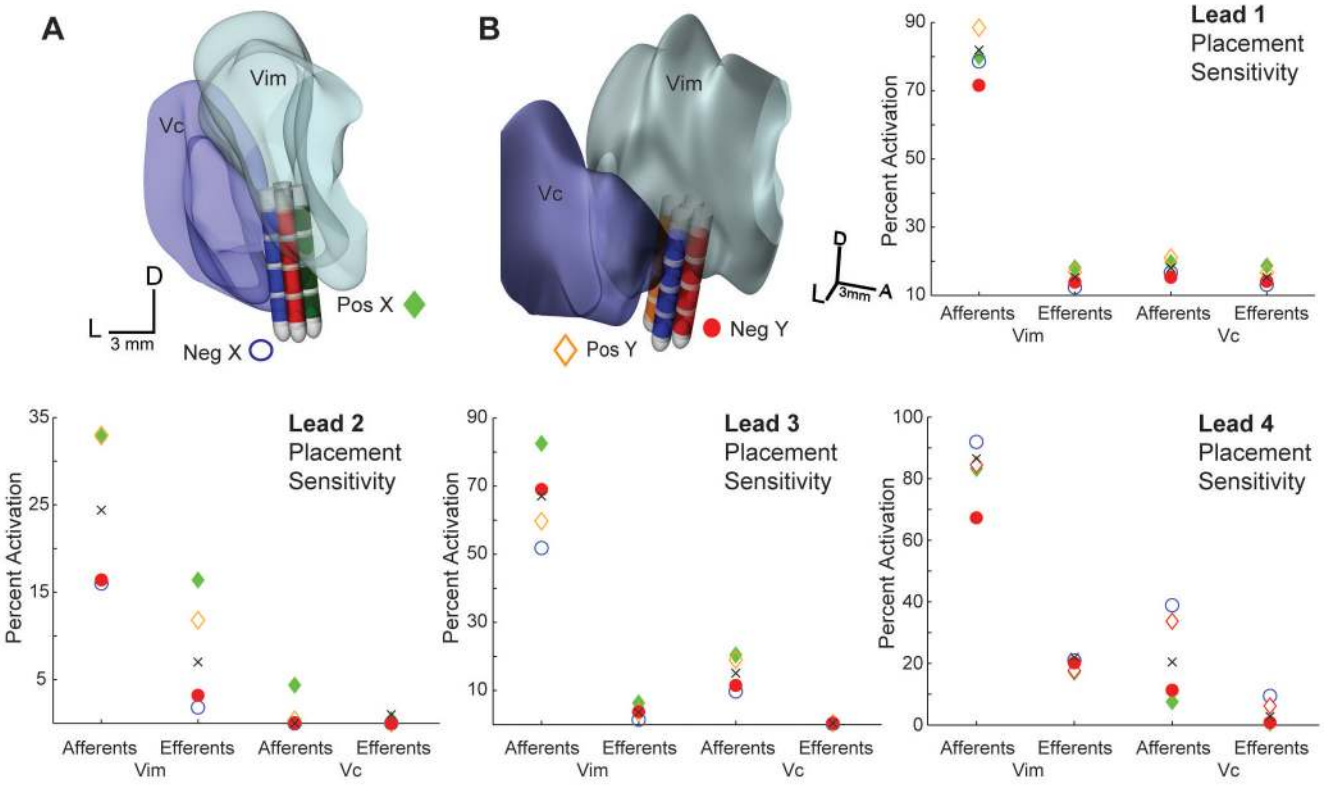

Figure 5.

Sensitivity analysis of lead placement was performed by shifting the DBS lead 1 mm in each direction of the stereotactic microdrive plane. An example of this manipulation is illustrated in **A)** and **B)** for Subject 3 (Lead 4). Plots show model predictions for percent activation of the afferent and efferent pathways after shifting the DBS lead in each direction (blue-negative x, green-positive x, orange-positive y, red-negative y). The black x marker indicates the original model predictions for the clinician-optimized bipolar DBS setting.

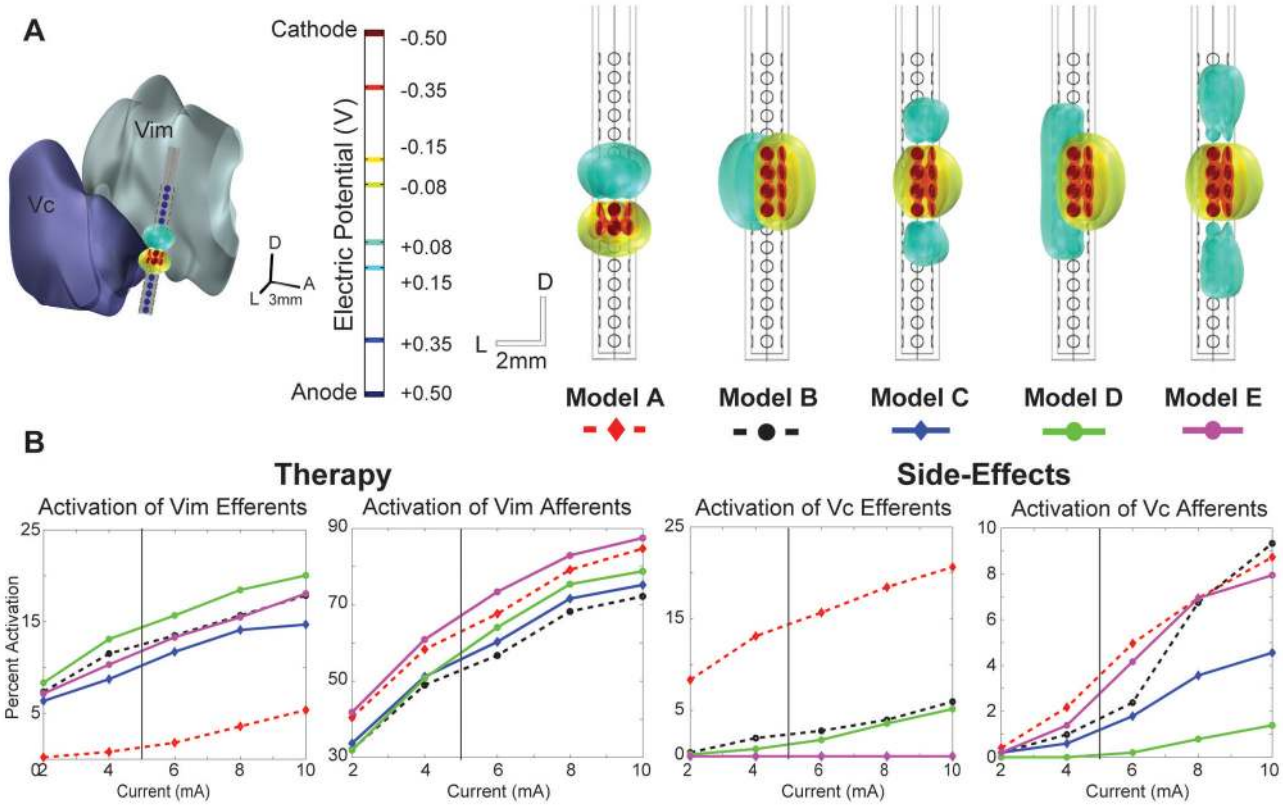

Figure 6.

Five dDBS stimulation configurations were evaluated in place of the cylindrical lead for Subject 3 (Lead 4), who never achieved complete suppression of tremor. **A)** dDBS lead configurations with isosurfaces illustrating the electric potential surrounding the lead. Cathodic contacts are indicated in red and anodic contacts in blue. Model A represents an estimated match between the dDBS lead and the bipolar setting finalized in the clinic. Models B-E maintained eight cathodic contacts oriented towards the Vim while the anodic contacts were shifted around the lead for assessment of optimized activation. The Vim is located anterior to the lead, and the Vc is located posterior to the lead. **B)** Activation plots of Vim and Vc efferents and afferents versus total current injection. The vertical bar represents the estimated equivalent voltage source stimulated in the final clinical setting.

Table 1

Programming details for each implanted DBS lead. All three DBS patients were programmed with a voltage-controlled, 185 Hz, 90 μs cathodic phase, continuous pulse train.

				Final DBS Setting				
Subject	**Age**	**Gender**	**Implant Side**	**Cathode**	**Anode**	**Pulse Width**	**Voltage**	**Frequency**
1	68	M	Left	2	Case	90 μs	2 V	185 Hz
2	76	M	Left	2	Case	90 μs	1 V	185 Hz
3	75	M	Left	1	Case	90 μs	2 V	185 Hz
			Right	2	3	90 μs	2.5 V	185 Hz